European Journal of Medicinal Chemistry 45 (2010) 5130–5139

Contents lists available at ScienceDirect

European Journal of Medicinal Chemistry

journal homepage: http://www.elsevier.com/locate/ejmech

Original article

Synthesis, characterization, oxidative degradation, antibacterial activity and acetylcholinesterase/butyrylcholinesterase inhibitory effects of some new phosphorus(V) hydrazides

Khodayar Gholivand [a,*], Zahra Hosseini [a], Sedigheh Farshadian [a], Hossein Naderi-Manesh [b]

[a] Department of Chemistry, Faculty of Science, Tarbiat Modares University, P.O. Box 14115-175, Tehran, Iran
[b] Department of Biochemistry and Biophysics, Faculty of Science, Tarbiat Modares University, Tehran, Iran

ARTICLE INFO

Article history:
Received 4 May 2010
Received in revised form
9 August 2010
Accepted 10 August 2010
Available online 18 August 2010

Keywords:
Phosphorus(V) hydrazide
Oxidative degradation
Antibacterial activity
Acetylcholinesterase/butyrylcholinesterase inhibitory

ABSTRACT

Some new phosphorus(V) hydrazides **1a**–**12a** were synthesized and characterized by ^{1}H, ^{13}C, ^{31}P NMR, IR spectroscopy and elemental analysis. Moreover, the interaction of $Cu(M)_2 \cdot nH_2O$ with **1a**, **3a** and **7a** gave 4,4′-bis(morpholine)diazene (**1b**). In fact, in these reactions, copper(II) ions acted as oxidizing agent. The results supported the proposed mechanism. The structures of compounds **1a**, **1b** and **1c** were further determined by X-ray crystallography. Compounds **1a**–**12a** were screened for their antibacterial activities. Also, the acetyl- and butyrylcholinesterase inhibitory activity of **1a**, **3a**, **7a**, **11a** and **12a** was measured using Ellman's method. It is interesting that these compounds were more potent inhibitors of BChE than of AChE. Also, using Lineweaver–Burk plots, it was indicated these compounds are mixed inhibitors.

1. Introduction

Hydrazides and hydrazones based on N-aminomorpholine and N-aminopiperidine are biologically active materials, in particular those which decrease the growth of malignant tumors [1,2] and are the intermediates for bulk drugs, linsidomine and molsidomine [3]. In recent years, there has been significant growth in the field of phosphorus acid hydrazides [4–7]. The presence of two nucleophilic nitrogen atoms together with the phosphorus atom in phosphorus acid hydrazides has led to extensive synthetic possibilities of these compounds. Substances with properties useful in practice have been discovered among them. Also, the hydrazides of phosphorothioic acid esters, diarylphosphinic acid esters of methylphosphonic and methylphosphonothioic acid exhibit pesticidal, bactericidal and fungicidal activities [8–10]. The inhibition of AChE by organophosphorus compounds is well documented [11–15], but investigations into the inhibition of BChE with organophosphorus compounds have been less systematic [16,17]. In our previous studies, we reported the inhibition potency of carbacylamidophosphates with general formula RC(O)NHP(O)(morpholine)$_2$; R = *p*-Cl, Br, Me, H–C_6H_4, CCl_3, CF_3, CH_2Cl and $CHCl_2$ on human erythrocyte acetylcholinesterase and bovine erythrocyte butyrylcholinesterase activity [18,19]. The results showed that the differences in the inhibition potencies of organophosphorus agents are a manifestation of differing molecular properties of the inhibitors involved in the interaction with the active site of the enzyme. To our knowledge, there are no reports in the literature of the cholinesterase inhibitory effects of hydrazinophosphorus derivatives containing P–N–N and N–N–P–N–N structures.

From the above consideration, and in connection with our current works in the field of phosphoramidate chemistry and their enzyme inhibitory effects [20,21], here we synthesized and characterized 12 new phosphorus(V) hydrazides based on N-aminomorpholine and N-aminopiperidine **1a**–**12a** as drawn in Scheme 1 and the crystal structure of compound **1a** was studied. Besides, the reactions of **1a, 3a** and **7a** with $CuM_2 \cdot nH_2O$ (M = Cl, NO_3, ClO_4, OAc) were considered and the crystal structure of the products (**1b** and **1c**) was determined.

Compounds **1a**–**12a** were screened for the antibacterial activity against *Bacillus subtilis*, *Bacillus cereus*, *Staphylococcus aureus*, *Escherichia coli*, *Pseudomonas aeruginosa* and *Klebsiella pneumonia*.

In addition, the inhibitory effects of **1a**, **3a**, **7a**, **11a** and **12a** on AChE and BChE activity were determined using a modified Ellman's method [22] and their inhibition mechanisms were evaluated by obtaining Lineweaver–Burk plots [23].

* Corresponding author. Tel.: +982182884422; fax: +982182883455.
E-mail address: gholi_kh@modares.ac.ir (K. Gholivand).

0223-5234/$ – see front matter © 2010 Elsevier Masson SAS. All rights reserved.
doi:10.1016/j.ejmech.2010.08.025

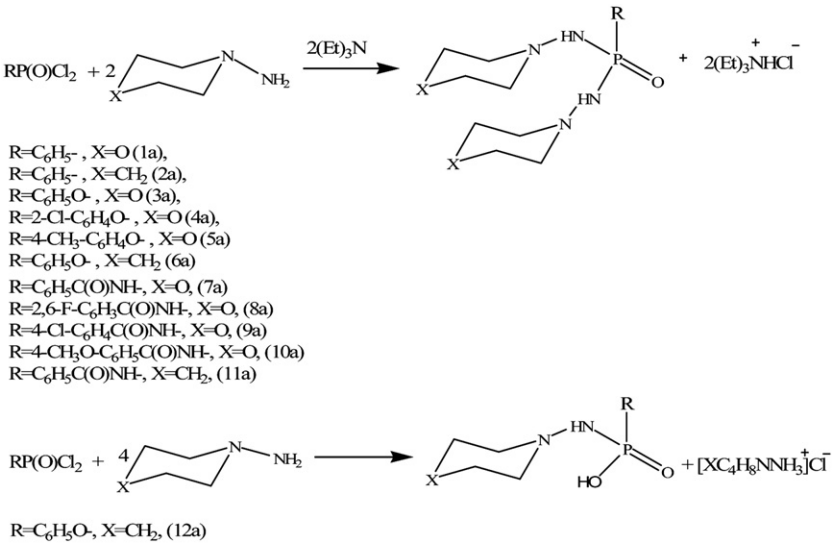

Scheme 1. The synthesis pathways of **1a**–**12a.**

2. Chemistry

2.1. Procedure for the synthesis of compounds (*1a*–*12a*)

N-Benzoyl phosphoramidic dichloride, 4-chloro-N-benzoyl phosphoramidic dichloride, 4-methoxy-N-benzoyl phosphoramidic dichloride 2,6-difluoro-N-Benzoyl phosphoramidic dichloride and (4-tolyl) dichlorophosphate were prepared according to the literature methods [24,25].

Compounds **1a**–**11a** were prepared by the reaction of 15 mmol phosphoric dichloride derivatives with 30 mmol of the corresponding amines in the presence of 30 mmol of triethylamine as HCl scavenger in dry tetrahydrofurane or acetonitrile. The temperature was controlled in the range −5 to −8 °C. After stirring for 8–14 h, the precipitate was filtered and the product was washed with cool acetone. Colorless crystals of **1a** were obtained by slow evaporation of acetone.

Compound **12a** was prepared by the reaction of 15 mmol phosphoric dichloride derivative with 60 mmol of the corresponding amine in dry acetonitrile at −5 to −8 °C. After stirring for 12 h, the precipitate was filtered and the solvent was evaporated to give the product that was washed with acetone.

2.2. Procedure for the oxidative degradation with $CuM_2 \cdot nH_2O$

$CuCl_2 \cdot 2H_2O$ (30 mg, 1 mmol) was dissolved in methanol (5 ml) and added to the solution of $C_6H_5P(O)(NH(NC_4H_8O))_2$ (**1a**) (107 mg, 2 mmol) in 10 ml methanol. The mixture was stirred at 70 °C for an hour and at room temperature for 48 h. Slow evaporation of the solution afforded crystalline material that consists of the mixture of crystals of 4,4′-bis(morpholine)diazene (**1b**), colorless prisms (60%), bis(morpholinium) tetrachlorocuprate (**1c**), green needles (20%) and $C_6H_5P(O)(OCH_3)_2$(**1d**) (20%). The crystals were separated manually. The reactions of $Cu(NO_3)_2 \cdot 6H_2O$, $Cu(ClO_4)_2 \cdot 6H_2O$ and $Cu(OOCCH_3)_2 \cdot 2H_2O$ with **1a** were also carried out and produced **1b** and **1d**. Additionally, the interaction of the solution of $CuCl_2 \cdot 2H_2O$ with the solution of **3a**, **7a**, and 4-aminomorpholine in methanol afforded the same colorless prism crystals of **1b**. Unfortunately, it was not possible to mimic the above reaction with other compounds.

3. Pharmacology

3.1. Antibacterial activity

The *in vitro* antibacterial activities of synthesized compounds were tested against six bacteria: three Gram-positive [*B. subtilis*, *B. cereus* and *S. aureus*] and three Gram-negative [*E. coli*, *P. aeruginosa* and *K. pneumonia*], by using the filter paper disc method [26] in nutrient agar medium. The bacteria were cultured in nutrient agar medium and used as inoculums. Whatmann filter paper discs (diameter 6.5 mm) were saturated with the solutions of test compound (concentration: 5, 10 mg ml^{-1}) or reference drug, chloroamphenicol (concentration: 5 and 10 mg ml^{-1}). The discs were incubated at 37 ± 1 °C for 20–24 h. The zone of inhibition of growth was measured, which indicates the inhibitory activity of the compounds on the growth of the bacteria. The average of three diameters was calculated for each sample.

3.2. AChE assay

Human acethylcholinesterase activity measurements were performed essentially according to the method of Ellman. The reaction mixtures for determination of IC_{50} values, the median inhibitory concentration, consisted DTNB (5,5′-dithiobis(2-nitrobenzoic acid)) (10^{-4} M concentration) solution, 50 μl; inhibitor, x μl (5–250); acetylthiocholin iodide (ATCh) (1.35×10^{-4} M concentration) solution, 30 μl; 70 mM phosphate buffer (Na_2HPO_4/NaH_2PO_4, pH = 7.4) ($885 - x$) μl and hAChE (20 μl volume, diluted 100 times in phosphate buffer solution, 30 μl). The absorbance change at 37 °C was monitored with the spectrophotometer at 412 nm for 3 min and three replicates were run in each experiment. In the absence of inhibitor, the absorbance change was directly proportional to the enzyme level. The plot of V_I/V_0 (V_I and V_0 are the activity of the enzyme in the presence and absence of inhibitors, respectively) against log [I], where [I] is the inhibitor concentration, gave the IC_{50} values of compounds **1a**, **3a**, **7a**, **11a** and **12a** (Figs. 1 and 2). K_m and V_{max} values were determined in the absence and presence of inhibitor from the double reciprocal Lineweaver–Burk plots (Figs. 3–5).

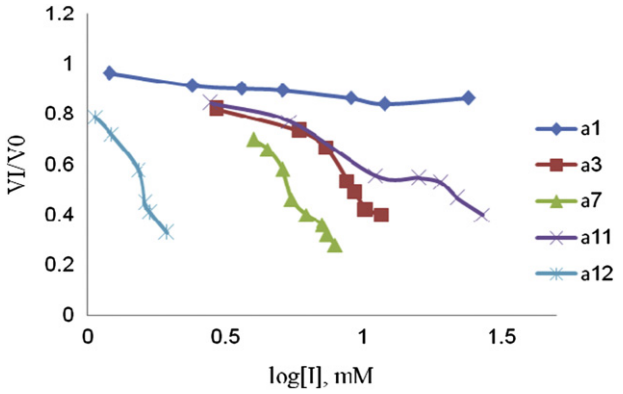

Fig. 1. The plot of V_I/V_0 against (log[I], mM) for inhibitors **1a**, **3a**, **7a**, **11a** and **12a**. V_I and V_0 are the acetylcholinesterase enzyme activity (OD min^{-1}) and [I] is the inhibitor concentration (mM).

3.3. BChE assay

The activity of BChE was determined the same as AChE activity by measuring thiocholine which reacted with DTNB after hydrolysis of BTCh. The lyophilized BChE was diluted with 100 mM phosphate buffer (pH = 8) for using in activity assay.

3.4. Hydrophobic parameter evaluation

Calculated log P, hydrophobicity extent, of compounds **1a**, **3a**, **7a**, **11a** and **12a** were performed using software log P, chemdraw Ultra, 8.0.3, 2003.

4. Results and discussion

4.1. Spectral study

Structural assignment of **1a**–**12a** was carried out using IR, ^{31}P, ^{1}H, ^{13}C NMR spectroscopy and the results are summarized in Table 1. In **7a**–**11a**, as we observed earlier for phosphoramidate analogues [27], the P–N_{amine} stretching vibrations (1002–1017 cm^{-1}) appear at higher frequencies than the P–N_{amide} vibrations (902–920 cm^{-1}). The N–N vibrational frequencies are observed in the range of 911–948 cm^{-1}. A comparison between similar compounds **1a**–**11a** indicate that the $\nu_{P=O}$ in compounds with X = O in amino ring moieties is stronger than compounds with X = CH_2. ^{1}H NMR spectra of **1a**–**12a** show the coupling constants $^{2}J(PNH)_{amine}$ between phosphorus atom and the α proton of the hydrazino group in the range of 25.2–35.0 Hz. As shown in Table 1, in compounds with similar moieties, on decreasing the N–N vibrational frequencies in IR spectra, the $^{2}J(PNH)_{amine}$ values become greater approximately. The ^{31}P chemical shifts show when Ph–P linkage changes to Ph–O–P in **1a** and **2a**; Ph–C(O)NH–P in compounds **3a**–**11a**, C(O)NH groups cause more deshielding of the phosphorus atom. Also, the ^{31}P chemical shifts of **2a**, **6a** and **11a** with aminopiperidine derivatives appear in upfield compared with their isostructures, **1a**, **3a** and **7a** with aminomorpholine derivatives. The carbons with one bond distance from the N atom in all of the synthesized compounds are equivalent and $^{3}J(P,C_{aliphatic})$ values vary between 4.5 and 10.0 Hz (Table 1). For *ipso* carbon atoms of phenyl rings, $^{n}J(P,C_{aromatic})$ are 153.4 and 152.0 Hz ($n = 1$) in **1a** and **2a**; 6.6–4.7 Hz ($n = 2$) in **3a**, **4a**, **5a**, **6a** and **12a**; 4.5 and 7.9 Hz ($n = 3$) in **7a** and **11a** respectively.

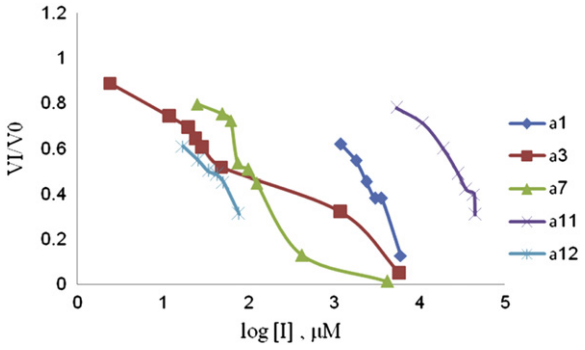

Fig. 2. The plot of V_I/V_0 against (log[I], µm) for inhibitors **1a**, **3a**, **7a**, **11a** and **12a**. V_I and V_0 are the butyrylcholinesterase enzyme activity (OD min^{-1}) and [I] is the inhibitor concentration (µm).

The mass spectra of **1a** and **9a** showed the existence of fragmentation at $m/z = 101$ and 86, which belong to $C_4H_9N_2O^+$ and $C_4H_8NO^+$ cations with high intensity, respectively, that the latter attributed to the break of N–N bond.

4.2. X-ray crystallography investigation

Single crystals were obtained from a solution of acetone (for **1a**) and methanol (for **1b** and **1c**) after slow evaporation at room temperature. The crystal data and the details of the X-ray analysis are given in Table 2, selected bond lengths and angles of **1a** and **1b** are given in Tables 3 and 4 respectively. The molecular structure of **1a** is shown in Fig. 6. It is interesting to note that the P=O bond distance is considerably lengthened in comparison to the normal P=O bond length (1.45 Å) (Table 2). Also, the P–N_{amine} bond lengths are shorter than P–N single bond length (1.77 Å) and longer than P–N double bond length (1.57 Å), in agreement with similar compounds reported in the literature [28]. The coordination environment around the central phosphorus atom of **1a** is largely tetrahedral. The morpholine moiety adopts a chair conformation with tetrahedral nitrogen atoms (N2 and N4). In most phosphinoamines, the P–N bonded nitrogen is planar, but the structural feature of interest in **1a** is the presence of pyramidalized nitrogen atoms ($\sum\angle$N(1) and N(3) are 355.57 and 347.39° respectively). This pyramidal nitrogen center was previously observed in some organophosphonic diamides [29]. The observed N–N distances (1.422 (2), 1.434(2) Å) show slightly multiple bonding character. The data of hydrogen bonding are presented in Table 5. The two N–H and phosphoryl groups on each molecule are involved in intermolecular hydrogen bonding with two neighboring molecules and one dimensional polymeric structures shown in Fig. 7 along the *a* axis are obtained.

The molecular structure of **1b** is shown in Fig. 8. The selected bond lengths and angles are given in Table 4. The torsion angle of tetrazene (N1–N2–N2–N1 = 180.0°) shows that the molecular structure is exactly E configuration about the azo (N2=N2A) bond, however in 2,5,2′-triazido-1,1′-azo-1,3,4-triazole [30] and 1,4-bis-[1-methyl-tetrazol-5-yl]-1,4-dimethyl-2-tetrazene [31] this angle was 177.8(2)°. The sum of N(2)–N(1)–C(1), N(2)–N(1)–C(2), C(1)–N(1)–C(4) bond angle is 339.21°, therefore, the atoms N(1) and N(1A) are sp^3 hybridized. The bond length of the N1–N2 is 1.3950 (11) Å in **1b**, which is shorter than the accepted N–N single bond length (1.44 Å). Also, the bond length between the N atoms of the azo group (N2=N2A) is 1.2556(17) Å, which is the same for the accepted N–N double bond length (1.25 Å). In fact, there is a localization of the azo π electrons along the N2 moiety within **1b**.

The crystal structure of bis(morpholinium) tetrachlorocuperate (**1c**) was previously determined [32] at 22 °C. We report here a redetermination of **1c**, at low temperature (120(2) K), in good agreement with previous study and its packing diagram is presented in Fig. 9.

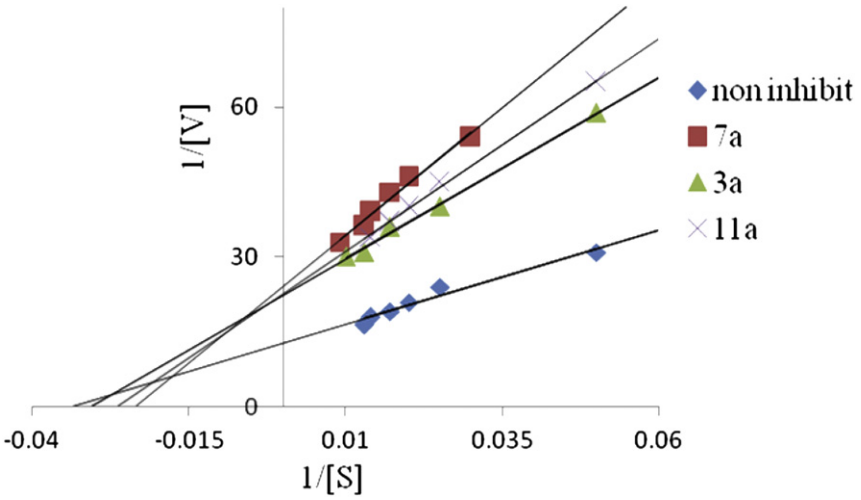

Fig. 3. The plot of 1/[V] against 1/[S] for inhibitors **3a, 7a**, **11a** and acetylcholinesterase activation without inhibitor. [V] is the enzyme activity (OD min^{-1}) and [S] is the ATCh concentration (mM).

4.3. Oxidative degradation results

Phosphoryl-containing compounds have been used as effective complexation agents in coordination chemistry [33–36]. In this paper, our aim was the coordination of synthesized phosphorus(V) hydrazides to Cu(II) ion due to the biological properties of Cu(II) complexes [37]. Unexpectedly, the reaction of 2 equiv PhP(O)(NH$(NC_4H_8O))_2$ (**1a**) with 1 equiv of $CuCl_2{\cdot}2H_2O$ afforded 4,4′-bis (morpholine)diazene (**1b**), bis(morpholinium) tetrachlorocuprate (**1c**) and dimethyl phenyl phosphonic acid (**1d**).

N-Unsubstituted hydrazides of phosphorus diesters were previously oxidized by iodine in aqueous solutions in the presence of tertiary amines with liberation of nitrogen and the formation of phosphoric acid diesters [38]. In addition, the oxidation of phosphorodi(N,N-alkylarylamidic) 2-methoxy(ethoxy)carbonylhydrazides with lead tetraacetate led to the formation of the corresponding azo-derivative [39]. Also, the oxidation of N-aminomorpholine by use of benzeneseleninic acid [40], manganese dioxide [41] and hexamethyldisilane [42] as oxidizing agents afforded **1b** in the moderate yield, whereas in this work, **1b** was prepared by copper ion as oxidizing agent with high yield. 2-Tetrazenes are composed of a four nitrogen chain with a central double bond and they are widely applicable. For example, they serve as chain-transfer agents in vinyl polymerization [43], source of free amine radicals [44] and anticancer agents [45]. Scheme 2 depicts our proposed mechanism for the oxidative degradation of candidate phosphorus(V) hydrazides to tetrazene by use of Cu (II) under methanol solvent. The first step was the nucleophilic substituent reaction of phosphorus(V) hydrazide (I) to phosphorus acid ester (II). The second step involved the removal of hydrogen atoms from 4-aminomorpholine by $CuCl_2{\cdot}2H_2O$ giving rise the aminonitrene(III), which finally the formation of the tetrazene is explained in terms of the dimerization of the aminonitrene. It seems that the formation of **1c** takes place in a competitive mechanism with above proposed mechanism.

4.4. Antibacterial activity results

The antibacterial results are given in Table 6. The antibacterial activity is directly proportional to the concentration of the tested compounds. It may be concluded that as the concentration is increased, these compounds inhibit the growth of bacteria to a greater extent. The most sensitive bacterial species on compounds tested is Gram-positive bacteria, *S. aureus* and *E. coli*, while Gram-negative bacteria *P. aeruginosa* is the most resistant species and only **12a** exhibits antibacterial activity toward it. The compounds containing aminopiperidine substituents have more activity toward tested bacteria than their isostructural compounds containing aminomorpholine substituents. Comparing the obtained results to the standard antibiotic, chloramphenicol, 1**2a** has stronger antibacterial effect against *P. aeruginosa*.

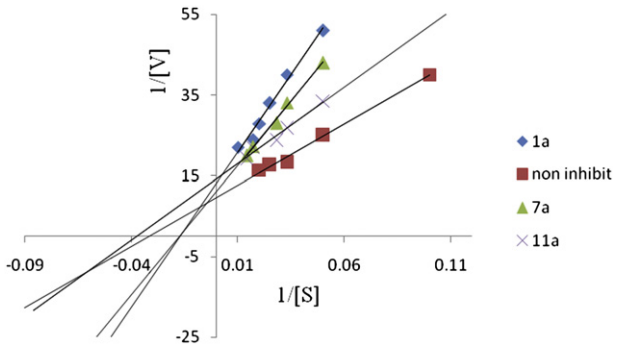

Fig. 4. The plot of 1/[V] against 1/[S] for inhibitors **1a**, **7a**, **11a** and butyrylcholinesterase activation without inhibitor. [V] is the enzyme activity (OD min^{-1}) and [S] is the BTCh concentration (mM).

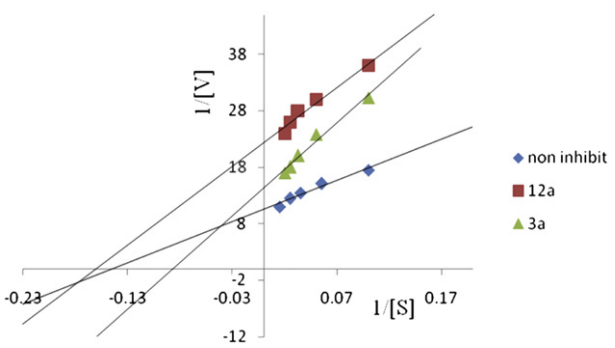

Fig. 5. The plot of 1/[V] against 1/[S] for inhibitors **3a**, **12a** and butyrylcholinesterase activation without inhibitor. [V] is the enzyme activity (OD min^{-1}) and [S] is the BTCh concentration (mM).

Table 1
IR vibration frequencies (cm^{-1}), ^{31}P chemical shifts (ppm) and coupling constants (Hz), of the synthesized compounds.

Comp.	P=O	C=O	P–N[a]	P–N[b]	N–H[a]	N–H[b]	N–N	$\delta^{31}P$	δNH[b]	$^2J_{(PNH)}$[b]	δNH[a]	$^2J_{(PNH)}$[a]	$^3J_{(PNC)}$	$^nJ_{(P,Cipso)}$
1a	1183	–	–	948	–	3435	990	15.77	5.81	25.2	–	–	10.0	153.4
2a	1185			910	–	3430	958	15.12	–	br	–	–	9.9	152.0
3a	1222	–	–	929	–	3445	902	6.78	6.32	35.0	–	–	5.2	6.6
4a	1193	–	–	914	–	3420	945	7.16	6.51	31.4	–	–	6.6	5.0
5a	1197	–	–	917	–	3455	956	6.87	6.27	31.3	–	–	5.1	4.8
6a	1222	–	–	920	–	3430	920	6.95	4.77	32.6	–	–	5.1	6.6
7a	1212	–	920	1009	3159	3355	970	4.72	4.74	27.0	8.86	5.2	4.8	0.0
8a	1207	1670	912	1010	3260	3445	925	0.25	5.99	30.5	9.62	6.6	4.5	0.0
9a	1219	1651	912	1011	2960	3265	970	2.31	4.74	27.0	9.20	5.0	4.6	8.6
10a	1211	1647	910	1002	3260	3420	936	2.88	5.99	30.5	9.02	0.0	4.7	0.0
11a	1211	1713	902	1017	3260	3265	926	2.49	5.63	30.0	9.08	0.0	4.4	7.9
12a	1171	–	–	876	–	3150	910	−4.49	4.11	br	–	–	4.8	4.8

[a] Amide.
[b] Amine.

4.5. AChE and BChE activity results

Enzymatic experiments on synthesized compounds were performed to illustrate the inhibition behavior and different biological activity characteristics of new derivatives of phosphoramidates. Values for the inhibitory activity of the compounds **1a**, **3a**, **7a**, **11a** and **12a** against AChE and BChE were expressed as IC_{50} and log *P* values are reported in Tables 7 and 8. The inhibition potency of the compounds indicates an increasing inhibitory effect on AChE: **11a** > **12a** > **3a** > **7a** and on BChE: **11a** > **12a** > **3a** > **7a** > **1a** as obtained by IC_{50} values comparison. The data demonstrate that **1a** gives no significant change in the activity of the AChE, but inhibits the activity of BChE. The inhibitory process of candidate compounds was compared with respect to hydrophobicity and electronic effects. It is well known that the hydrophobic character of organophosphorus compounds as operationally defined by octanol/water partition coefficient (log *P*) plays an important role in toxicity of them [46–48]. It is now quite clear that small difference in hydrophobic character can be important. The replacement of $-CH_2$-moiety by −O-moiety in amine substituents, increases the hydrophobicity. As we expected there is a linear relationship between IC_{50} values and hydrophobicity (log *P*) in isostructure compounds **1a**, **3a**, **7a** and **11a** with N–N–P–N–N structures, that is, as the IC_{50} values decrease, log *P* increase. It is revealed that hydrophobic substituents enhance the association of organophosphorus with AChE and BChE. The electropositivity of the phosphorus atom in the Coulombic association of the inhibitors with the active site serine of AChE is important. The ^{31}P chemical shift is one

Table 2
Crystal data collection and structure refinement parameters for compounds **1a, 1b** and **1c**.

Compound	**1a**	**1b**	**1c**
Formula	$C_{14}H_{23}N_4O_3P$	$C_8H_{16}N_4O_2$	$C_8H_{20}Cl_4CuN_2O_2$
Formula weight	326.33	200.25	381.60
Temperature (K)	120(2)	120(2)	120(2)
Wavelength (Å)	0.71073	0.71073	0.71073
Crystal system	Orthorhombic	Monoclinic	Orthorhombic
Space group	*Pna*21	*P*2(1)/c	*Pnma*
a (Å)	7.7634(12)	7.8668(13)	7.6201(4)
b (Å)	11.5332(15)	6.0462(10)	20.8219(11)
c (Å)	18.477(2)	10.7655(18)	9.1887(5)
α (deg)	90	90	90
β (deg)	90	109.940(3)	90
γ (deg)	90	90	90
V ($Å^3$)	1654.4(4)	481.36(14)	1457.92(13)
Z	4	2	4
D_{calc} ($Mg\,m^{-3}$)	1.310	1.382	1.739
Absorption coefficient (mm^{-1})	0.184	0.102	2.223
F(000)	696	216	780
Crystal size (mm)	0.21 × 0.17 × 0.15	0.17 × 0.12 × 0.08	0.451 × 0.354 × 0.128
Theta range for data collection (°)	2.08–29.49	2.75–28.99	1.96–26.97
Index ranges	$-6 \le h \le 10$ $-13 \le k \le 15$ $-21 \le l \le 25$	$-10 \le h \le 10$ $-8 \le k \le 8$ $-14 \le l \le 14$	$-9 \le h \le 9$ $-26 \le k \le 26$ $-11 \le l \le 11$
Reflections collected/unique (R_{int})	8893/4287(0.0357)	5058/1282 (0.0230)	13068/1443(0.0324)
Completeness to *θ* (%)	99.2	100.0	100.0
Absorption correction	Semi-empirical from equivalents	Semi-empirical from equivalents	Semi-empirical from equivalents
Maximum and minimum transmission	0.972 and 0.959	0.989 and 0.980	0.748 and 0.397
Refinement method	Full-matrix least-squares on F^2	Full-matrix least-squares on F^2	Full-matrix least-squares on F^2
Data/restraints/parameters	4287/1/200	7872/1/334	1636/0/82
Goodness-of-fit on F^2	1.002	0.997	1.011
Final *R* indices	$R1 = 0.0442$ wR2 = 0.0936	$R1 = 0.0436$ wR2 = 0.1154	$R1 = 0.0401$ $wR2 = 0.0940$
R indices (all data)	$R1 = 0.0574$ $wR2 = 0.0989$	$R1 = 0.0488$ $wR2 = 0.1230$	$R1 = 0.0450$ $wR2 = 0.0982$
Largest difference in peak and hole ($e\,Å^{-3}$)	0.493 and −0.269	0.268 and −0.282	1.078 and −1.117

Table 3
Selected bond lengths and bond angels for **1a**.

Bond	Distance (Å)	Bond	Distance (Å)
P(1)–O(1)	1.4975(14)	N(1)–N(2)	1.422(2)
P(1)–N(1)	1.6402(17)	N(1)–H(1N)	0.9000
P(1)–N(3)	1.6449(19)	N(3)–N(4)	1.434(2)
P(1)–C(9)	1.809(2)	N(3)–H(3N)	0.9000
Angle	Amplitude (°)	Angle	Amplitude (°)
O(1)–P(1)–N(1)	109.02(8)	N(1)–N(2)–C(4)	111.69(16)
O(1)–P(1)–N(3)	118.19(10)	N(1)–N(2)–C(1)	109.42(17)
N(1)–P(1)–N(3)	106.71(10)	C(4)–N(2)–C(1)	109.76 (17)
O(1)–P(1)–C(9)	110.65(10)	N(4)–N(3)–P(1)	116.89(15)
N(1)–P(1)–C(9)	111.56(10)	N(4)–N(3)–H(3N)	116.8
N(3)–P(1)–C(9)	100.45(11)	P(1)–N(3)–H(3N)	113.7
N(2)–N(1)–P(1)	117.87(13)	N(3)–N(4)–C(5)	108.01(17)
N(2)–N(1)–H(1N)	121.2	N(3)–N(4)–C(8)	110.70(18)
P(1)–N(1)–H(1N)	116.5	C(5)–N(4)–C(8)	109.17(17)

of the factors that can indicate electron density around phosphorus nuclei. It might be expected that the inhibitory of **1a**, with the least electron density around phosphorus nuclei (δ $^{31}P = 15.77$ ppm), should be larger than the others. However, as shown in Tables 7 and 8, this compound has no activity against AChE and less inhibition potency on BChE. Also, **12a** with the high electronegativity of phosphorus atom (δ $^{31}P = -4.49$ ppm) has more activity against AChE and BChE. Therefore ^{31}P NMR spectra are inadequate to explain the relationship between IC_{50} and the ^{31}P chemical shifts of these compounds. By comparing the IC_{50} values of Tables 7 and 8, it is clear that the inhibitory effects of these compounds are nearly 4- to 9-fold higher on BChE than on AChE.

Early hypotheses and modeling experiments indicated that the main functional difference between the AChE and BChE active sites is related to the structure of the acyl pocket [49]. Due to a larger substrate-binding pocket that can be accommodate bulky substrates [50], the specificity of BChE is much larger than that of AChE. It is interesting that compounds **11a** and **12a** with more hydrophobicity due to bulky aminopiperidine substituent have a stronger inhibitory effect on BChE than AChE.

The dependence of inhibitory potency and substrate concentration was studied initially in a classical way in order to determine the mechanism of inhibition. In Figs. 3–5, double reciprocal plots for candidate compounds yielded increasing slopes and intercepts, indicating the inhibitors are mixed ones. In these plots, *y*-intercept $= 1/V_{max}$, *x*-intercept $= -1/K_m$ and regression coefficients are between 0.91 and 0.99. The K_m and V_{max} values of these compounds and AChE and BChE are obtained under experimental conditions (Tables 7 and 8). The K_m's for ATCh and BTCh are 0.083 mM and 0.11 mM, respectively. The patterns of lines reveal that the plots for varying inhibitor concentrations depend on the value of α. The double reciprocal plots for compounds **3a**, **7a**, **11a** and **12a** with AChE show that in these compounds, the lines are intersect at a value of 1/[S] less than zero on the *x*-axis and a value of 1/[V] of greater than zero (Fig. 3) and $\alpha > 1$. In compounds **11a** and **12a** with BChE, the lines intersect below the *x* and *y* axes, at negative values of 1/[S] and 1/[V], where $\alpha < 1$ (Figs. 4 and 5).

Table 4
Selected bond lengths and bond angels for **1b**.

Bond	Distance (Å)	Bond	Distance (Å)
N(1)–N(2)	1.3950(11)	N(1)–C(4)	1.4671(12)
N(1)–C(1)	1.4637(13)	N(2)–N(2)#1	1.2556(17)
Angle	Amplitude (°)	Angle	Amplitude (°)
N(2)–N(1)–C(1)	118.05(8)	C(1)–N(1)–C(4)	112.10(8)
N(2)–N(1)–C(4)	109.06(8)	N(2)#1–N(2)–N(1)	112.99(10)

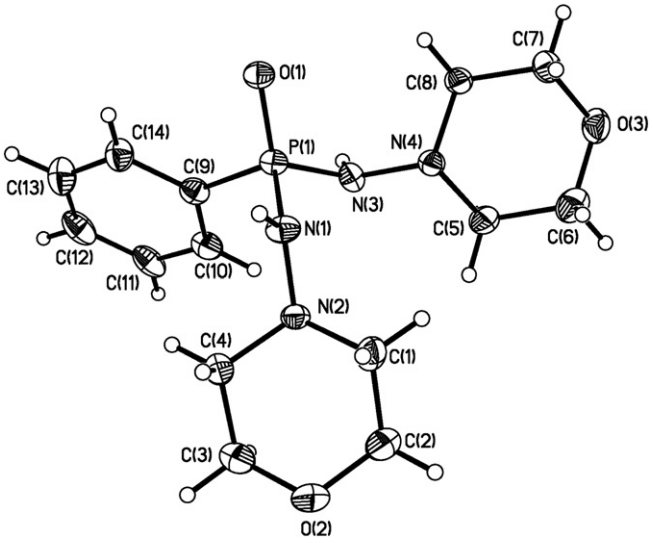

Fig. 6. Molecular structure of **1a** with numbering (50% probability ellipsoids).

5. Conclusion

In summary, some new phosphorus(V) hydrazides **1a**–**12a** based on N-aminomorpholine and N-aminopiperidine were reported. Also, the interaction of methanol solution of Cu $(M)_2 \cdot nH_2O$ (M = Cl, NO_3, ClO_4, OAc) with **1a**, **3a** and **7a** gave 4,4′-bis (morpholine)diazene (**1b**). The structures of compounds **1a**, **1b** and **1c** were further determined by X-ray crystallography. Compounds **1a**–**12a** were screened for their *in vitro* antibacterial activities against six bacteria. From the activity studies, it was concluded that *S. aureus* and *E. coli* were the most sensitive species. Also, the compounds bearing aminopiperidine moiety, exhibited better activities toward tested bacteria than those bearing amino-morpholine moiety. The inhibitory potencies of **1a**, **3a**, **7a**, **11a** and **12a** against human acetyl- and butyrylcholinesterase were studied. The data demonstrated these compounds were shown to be potent inhibitors of BChE versus AChE, respectively and **11a** and **12a** having aminopiperidine substituents have a stronger inhibitory effect on BChE than AChE. Also, these compounds were found to be mixed type of inhibitors.

6. Experimental

6.1. Spectroscopic measurements

All reactions were performed under an argon atmosphere and in dry solvents. ^1H, ^{13}C and ^{31}P NMR spectra were recorded on a Bruker Avance DRS 500 spectrometer. ^1H and ^{13}C chemical shifts were determined relative to internal TMS and ^{31}P chemical shifts relative to 85% H_3PO_4 as an external standard. Infrared (IR) spectra were recorded on a Shimadzu model IR-60 spectrometer. Elemental analysis was performed using a Heraeus CHN-O-RAPID apparatus. Mass spectra were obtained on a MS Model 5973 Network apparatus at ionization potential of 20 eV. Melting points

Table 5
Hydrogen bonds for compound **1a** (Å, °).

Complex	D–H–A	*d*(D–H)	*d*(H···A)	*d*(D···A)	<DHA
1a	N(1)–H(1N)···O(1) [$x+1/2, -y+1/2, z$]	0.90	2.12	3.002(2)	168
	N(3)–H(3N)···O(1) [$x-1/2, -y+1/2, z$]	0.90	2.04	2.900(2)	159

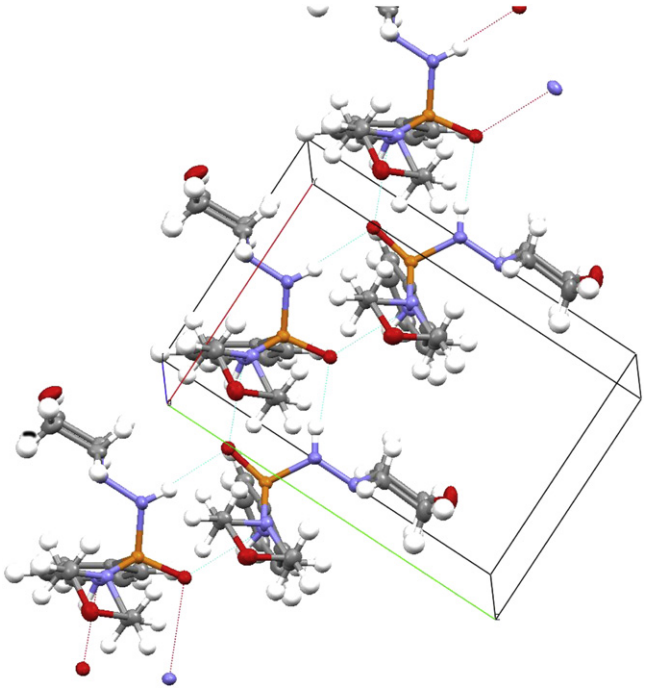

Fig. 7. A view of the unit cell packing of **1a**.

were obtained with an Electrothermal instrument. UV measurements were recorded on a Shimadzu UV-2100 spectrometer.

6.2. X-ray measurements

X-ray data of compounds **1a**, **1b** and **1c** were collected on a Bruker SMART 1000CCD [51] with graphite monochromated Mo Kα radiation ($\lambda = 0.71073$ Å). The structures were solved by the direct method using the SHELX-97 program package [52]. The non-hydrogen atoms were refined anisotropically and all located from subsequent difference Fourier maps and refer to final *R* values of 0.0442, 0.0436 and 0.0401 for **1a**, **1b** and **1c**, respectively.

Crystallographic data for the structures reported in this paper have been deposited with the Cambridge crystallographic data center as supplementary publication No. CCDC-727884 ($C_{14}H_{23}N_4O_3P$), CCDC-742026 ($C_8H_{16}N_4O_2$) and CCDC-742027 ($C_8H_{20}Cl_4Cu_1N_2O_2$). Copies of the data can be obtained free of charge on application to CCDC, 12 Union Road, Cambridge CB2 1EZ UK (fax: +44 1223 336033; e-mail: deposit@ccdc.cam.ac.uk).

6.3. N,N′-Bis(4-aminomorpholine) phenylphosponic diamide (*1a*)

Yield: 73%. M.p. = 196 °C. Anal. Calc. for $C_{14}H_{23}N_4O_3P$ (326.33): C, 51.48; H, 7.04; N, 17.16; Found: C, 51.50; H, 7.00; N, 17.50%.

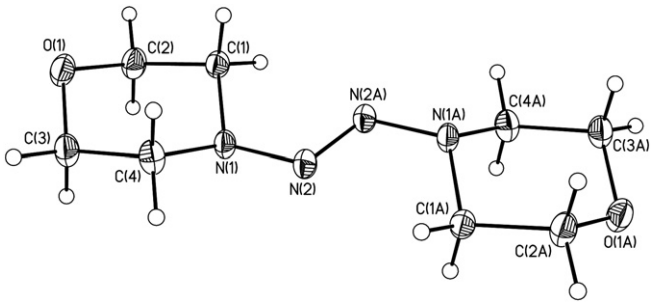

Fig. 8. Molecular structure of **1b** with numbering (50% probability ellipsoids).

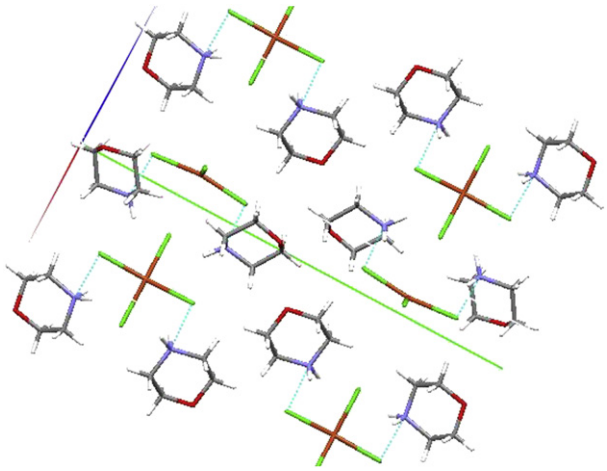

Fig. 9. A view of the unit cell packing of **1c**.

^{31}P NMR (202.46 MHz, d_6-DMSO, ppm): $\delta = 15.77$ (m). ^{1}H NMR (500.13 MHz, d_6-DMSO, ppm): $\delta = 7.82$ (d, $^3J_{P,H} = 11.2$ Hz, 2H; Ar–H), 7.48 (t, $^3J_{H,H} = 7.3$ Hz, 1H; Ar–H), 7.42 (t, $^4J_{P,H} = 3.1$ Hz, 2H; Ar–H), 5.81 (d, $^2J_{PNH} = 25.2$ Hz; NH_{amine}), 3.77–2.98 (t, $^3J_{H,H} = 4.5$ Hz; 8H), 2.64–2.54 (t, $^3J_{H,H} = 4.2$ Hz; 8H). ^{13}C NMR (125.77 MHz, d_6-DMSO, ppm): $\delta = 57.7$ (d, $^3J_{P,C} = 10.0$ Hz), 63.24 (s), 65.42 (s), 66.1 (s), 127.52 (d, $^2J_{P,C} = 12.6$ Hz), 130.81, 131.85 (d, $^3J_{P,C} = 7.6$ Hz), 132.87 (d, $^1J_{P,C} = 153.4$ Hz; C_{ipso}). IR (KBr, ν, cm^{-1}): 3435(w, br, N–H), 3055 (m, C–$H_{aromatic}$), 1435 (m, P–Ph), 1318–1358 (w, Ph), 1183 (s, P=O), 990 (w, N–N), 948 (s, P–N_{amine}).

6.4. N,N′-Bis(4-aminopiperidine) phenylphosponic diamide (*2a*)

Yield: 43%. M.p. = 232 °C. Anal. Calc. for $C_{16}H_{27}N_4OP$ (322.43): C, 59.55; H, 8.37; N, 17.36; Found: C, 59.50; H, 8.31; N, 17.50%. ^{31}P NMR (202.46 MHz, d_6-DMSO, ppm): $\delta = 15.29$ (m). ^{1}H NMR (500.13 MHz, d_6-DMSO, ppm): $\delta = 7.80$ (d, $^3J_{P,H} = 10.0$ Hz, 2H; Ar–H), 7.68 (m, 1H; Ar–H), 7.37 (m, 2H; Ar–H), 5.85 (br, NH_{amine}), 3.1 (m, 8H), 1.6 (m, 8H), 1.5 (m, 2H), 1.4 (m, 2H). ^{13}C NMR (125.77 MHz, d_6-DMSO, ppm): $\delta = 23.6$, 24.9, 53.91 (d, $^3J_{P,C} = 9.9$ Hz), 127.91 (d, $^2J_{P,C} = 12.2$ Hz), 129.11, 132.61 (d, $^3J_{P,C} = 6.5$ Hz), 133.39 (d, $^1J_{P,C} = 152.3$ Hz; C_{ipso}). IR (KBr, ν, cm^{-1}): 3430 (w, br, N–H), 3140 (m, C–$H_{aromatic}$), 1450 (m, P–Ph), 1185 (s, P=O), 958 (w, N–N), 910 (m, P–N_{amine}).

6.5. N,N′-Bis (4-aminomorpholine) phosphoramidic acid phenyl ester (*3a*)

Yield: 60%. M.p. = 160 °C. Anal. Calc. for $C_{14}H_{23}N_4O_4P$ (342.33): C, 49.08; H, 6.70; N, 16.36; Found: C, 49.10; H, 6.70; N,16.40%. ^{31}P NMR (202.46 MHz, d_6-DMSO, ppm): $\delta = 6.78$ (m). ^{1}H NMR (500.13 MHz, d_6-DMSO, ppm): $\delta = 7.32$ (t, $^3J_{H,H} = 8.8$ Hz, 2H; Ar–H), 7.21 (d, $^3J_{H,H} = 8.8$ Hz, 2H; Ar–H), 7.1 (t, $^3J_{H,H} = 7.2$ Hz, 1H), 6.32 (d, $^2J_{PNH} = 35.0$ Hz, 2H; NH_{amine}), 3.51 (m, 8H), 2.60 (t, $^3J_{H,H} = 4.7$ Hz, 8H). ^{13}C NMR (125.77 MHz, d_6-DMSO, ppm): $\delta = 57.80$ (d, $^3J_{P,C} = 5.2$ Hz; 4C), 66.1 (s), 120.2 (d, $^3J_{P,C} = 4.8$ Hz), 123.55, 129.23, 151.55 (d, $^2J_{P,C} = 6.6$ Hz; C_{ipso}). IR (KBr, ν, cm^{-1}): 3445 (w, br, N–H), 3285 (m, C–$H_{aromatic}$), 1453 (m, P–Ph), 1222 (s, P=O), 929 (s, P–N_{amine}), 902 (w, N–N).

6.6. 2-Chloro-N,N′-bis (4-aminomorpholine) phosphoramidic acid phenyl ester (*4a*)

Yield: 40%. M.p. = 185 °C. Anal. Calc. for $C_{14}H_{22}ClN_4O_4P$ (376.77): C, 44.58; H, 5.83; N, 14.86; Found: C, 44.10; H, 5.75; N, 14.80%. ^{31}P

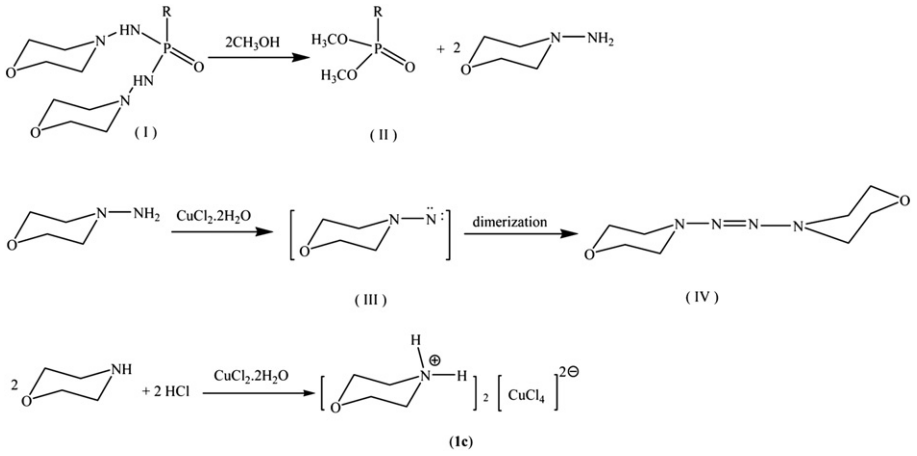

Scheme 2. The oxidative degradation process of **1a**, **3a** and **7a**.

NMR (202.46 MHz, d_6-DMSO, ppm): $\delta = 7.16$ (m). ^{1}H NMR (500.13 MHz, d_6-DMSO, ppm): $\delta = 7.59$ (d, $^3J_{H,H} = 8.2$ Hz, 1H; Ar–H), 7.41 (d, $^3J_{H,H} = 8.0$ Hz; 1H; Ar–H), 7.23 (t, $^3J_{H,H} = 7.55$ Hz; 1H; Ar–H), 7.01 (t, $^3J_{H,H} = 7.6$ Hz; 1H; Ar–H), 6.86 (d, $^2J_{PNH} = 31.4$ Hz, 2H; NH_{amine}), 3.54 (m, 8H), 2.49 (m, 4H), 2.24 (m, 4H). ^{13}C NMR (125.77 MHz, d_6-DMSO, ppm): $\delta = 20.20$, 57.70 (d, $^3J_{P,C} = 6.63$ Hz), 66.1, 120.2 (d, $^2J_{P,C} = 5.0$ Hz; C_{ipso}), 123.55, 129.23, 151.55. IR (KBr, ν, cm^{-1}): 3420 (w, br, N–H), 3165 (m, C–$H_{aromatic}$), 1477 (m, P–Ph), 1350–1390 (w, Ph), 1193 (m, P=O), 940 (w, N–N), 914 (m, P–N_{amine}), 768 (m, C–Cl).

6.7. N,N′-Bis (4-aminomorpholine) phosphoramidic acid (4-methyl-phenyl) ester (**5a**)

Yield: 60%. M.p. = 182 °C. Anal. Calc. for $C_{15}H_{25}N_4O_4P$ (356.36): C, 50.51; H, 7.01; N, 15.71; Found: C, 50.50; H, 7.00; N, 15.49%. ^{31}P NMR (202.46 MHz, d_6-DMSO, ppm): $\delta = 6.86$ (m). ^{1}H NMR (500.13 MHz, d_6-DMSO, ppm): $\delta = 7.06$–7.16 (m, 4H; Ar–H), 6.28 (d, $^2J_{PNH} = 31.3$ Hz, 2H; NH_{amine}), 3.51 (m, 8H), 2.60 (m, 8H). ^{13}C NMR (125.77 MHz, d_6-DMSO, ppm): $\delta = 57.76$ (d, $^3J_{P,C} = 5.1$ Hz), 66.0, 119.9 (d, $^3J_{P,C} = 4.8$ Hz), 129.55, 129.91, 149.31 (d, $^2J_{P,C} = 6.3$ Hz; C_{ipso}). IR (KBr, ν, cm^{-1}): 3455 (w, br, N–H), 3185 (m, C–$H_{aromatic}$), 1303–1381 (w, Ph), 1197 (s, P=O), 956 (w, N–N), 917 (s, P–N_{amine}).

6.8. N,N′-Bis (4-aminopiperidine) phosphoramidic acid phenyl ester (**6a**)

Yield: 75%. M.p. = 138 °C. Anal. Calc. for $C_{16}H_{27}N_2O_2P$ (310.12): C, 61.91; H, 8.71; N, 9.03; Found: C, 61.89; H, 8.70; N,9.01%. ^{31}P NMR (202.46 MHz, d_6-DMSO, ppm): $\delta = 6.95$ (m). ^{1}H NMR (500.13 MHz, d_6-DMSO, ppm): $\delta = 7.32$ (t, $^3J_{H,H} = 10.7$ Hz, 2H; Ar–H), 7.18 (d, $^3J_{H,H} = 10.0$ Hz, 2H; Ar–H), 7.08 (m, 1H), 6.00 (d, $^2J_{PNH} = 31.9$ Hz; NH_{amine}), 3.36 (m, 2H), 2.65 (t, $^3J_{H,H} = 5.2$ Hz; 6H); 1.25 (m, 4H). ^{13}C NMR (125.77 MHz, d_6-DMSO, ppm): δ =23.01, 25.50, 58.50 (d, $^3J_{P,C} = 5.1$ Hz), 120.24 (d, $^3J_{P,C} = 4.9$ Hz), 123.31, 129.11, 151.74 (d, $^2J_{P,C} = 6.6$ Hz; C_{ipso}). IR (KBr, ν, cm^{-1}): 3300 (w, br, NH), 3290 (m, C–$H_{aromatic}$), 1425 (s, P–Ph), 1337–1378 (w, Ph), 1222 (s, P=O), 920 (s, P–N_{amine}), 958 (w, N–N).

Table 6
Inhibition zone (mean diameter of inhibition in millimetres) as a criterion of antibacterial activities of the synthesized compounds.

Compound	Concentration (mg/ml)	*P. aeruginosa*	*E. coli*	*K. pneumonia*	*B. cereus*	*B. subtillus*	*S. aureus*
1a	5	–	–	–	–	–	–
	10	–	–	–	–	–	–
2a	5	–	–	–	–	–	–
	10	–	–	–	–	–	
3a	5	–	–	–	–	–	–
	10	–	–	–	–	–	–
4a	5	–	7	–	7	–	–
	10	–	10	–	10	–	–
5a	5	–	6	7	–	8	10
	10	–	11	14	–	18	13
6a	5	–	7	5	5	6	11
	10	–	15	15	14	13	17
7a	5	–	6	–	–	7	–
	10	–	11	–	–	13	8
8a	5	–	–	–	–	–	–
	10	–	–	–	–	–	–
9a	5	–	6	–	–	5	–
	10	–	13	–	8	12	–
10a	5	–	–	–	–	7	–
	10	–	7	–	7	13	–
11a	5	–	–	–	–	9	–
	10	–	–	–	–	19	7
12a	5	5	7	–	–	7	–
	10	10	11	–	–	15	8
Chloramphenicol	5	–	13	11	12	14	17
	10	7	17	15	15	17	22

Table 7
The enzymatic data for hAChE and candidate compounds

Compound	IC_{50} (mM)	log *P*	K_m (mM)	V_m (mM/min)	Inhibition mechanism
Enzyme	–	–	0.083	34.48	–
1a	–	−1.12	–	–	–
3a	9.55	−0.54	0.047	37.04	Mixed
7a	18.62	−0.78	0.049	55.55	Mixed
11a	1.95	1.35	0.045	40.01	Mixed
12a	5.49	1.29	0.051	11.11	Mixed

6.9. N-Benzoyl-N′,N″-bis (4-aminomorpholine) phosphoric triamide (**7a**)

Yield: 88%. M.p. = 177–179 °C. Anal. Calc. for $C_{15}H_{24}N_5O_4P$ (396.36): C, 45.41; H, 6.05; N, 17.66; Found: C, 45.10; H, 6.10; N, 17.60%. ^{31}P NMR (202.46 MHz, d_6-DMSO, ppm): $\delta = 4.72$ (m). ^1H NMR (500.13 MHz, d_6-DMSO, ppm): $\delta = 8.86$ (d, $^2J_{PNH} = 5.2$ Hz; $1H_{amide}$), 7.98 (d, $^3J_{H,H} = 7.8$ Hz, 1H; Ar–H), 7.58 (t, $^3J_{H,H} = 7.3$ Hz, 1H; Ar–H), 7.29 (t, $^3J_{H,H} = 7.5$ Hz, 2H; Ar–H), 4.74 (d, $^2J_{PNH} = 27.0$ Hz; NH_{amide}), 3.67 (m, 8H), 2.81 (m, 8H). ^{13}C NMR (125.77 MHz, d_6-DMSO, ppm): $\delta = 58.97$ (d, $^3J_{P,C} = 4.8$ Hz), 66.43, 131.97, 132.93, 133.43, 136.57, 169.63. IR (KBr, ν, cm^{-1}): 3400 (w, br, N–H), 3235 (m, C–$H_{aromatic}$), 1643 (vs, C=O), 1447 (m, C=C), 1421 (m, C–N_{amide}) 1212 (s, P=O), 1009 (m, P–N_{amine}), 920 (s, P–N_{amide}), 970 (w, N–N).

6.10. 2,6-Difluoro-N-benzoyl-N′,N″-bis (4-aminomorpholine) phosphoric triamide (**8a**)

Yield: 83%. M.p. = 212 °C. Anal. Calc. for $C_{15}H_{22}F_2N_5O_4P$ (432.36): C, 41.63; H, 5.09; N, 16.19; Found: C, 41.60; H, 6.00; N, 16.10%. ^{31}P NMR (202.46 MHz, d_6-DMSO, ppm): $\delta = 0.25$ (m). ^1H NMR (500.13 MHz, d_6-DMSO, ppm): $\delta = 9.62$ (d, $^2J_{PNH} = 6.6$ Hz; $1H_{amide}$), 7.49 (m, 2H), 7.14 (t, $^3J_{H,H} = 5.1$ Hz, 1H; Ar–H), 5.99 (d, $^2J_{PNH} = 30.5$ Hz; $2H_{amide}$), 3.56 (t, $^3J_{H,H} = 4.2$ Hz; 8H), 2.71 (m, 8H). ^{13}C NMR (125.77 MHz, d_6-DMSO, ppm): $\delta = 57.81$ (d, $^3J_{P,C} = 4.5$ Hz), 66.13, 111.9, 111.7. IR (KBr, ν, cm^{-1}): 3445 (w, br, N–H), 3260 (m, C–$H_{aromatic}$), 1671 (vs, C=O), 1463 (m, C=C), 1383 (m, C–N_{amide}) 1207 (s, P=O), 1010 (m, P–N_{amine}), 925 (w, N–N), 912 (m, P–N_{amide}).

6.11. 4-Chloro-N-benzoyl-N′,N″-bis (4-aminomorpholine) phosphoric triamide (**9a**)

Yield: 80%. M.p. = 201–205 °C. Anal. Calc. for $C_{15}H_{23}ClN_5O_4P$ (404.86): C, 44.45; H, 5.68; N, 17.29; Found: C, 44.10; H, 5.60; N, 17.30%. ^{31}P NMR (202.46 MHz, d_6-DMSO, ppm): $\delta = 2.31$ (m). ^1H NMR (500.13 MHz, d_6-DMSO, ppm): $\delta = 9.08$ (s, $^2J_{PNH} = 0.0$ Hz; $1H_{amide}$), 7.91 (d, $^3J_{H,H} = 8.5$ Hz, 2H; Ar–H), 7.54 (d, $^3J_{H,H} = 8.1$ Hz, 2H; Ar–H), 5.63 (d, $^2J_{PNH} = 30.0$ Hz; $2H_{amine}$), 3.53 (m, 8H), 2.67 (m, 8H). ^{13}C NMR (125.77 MHz, d_6-DMSO, ppm): $\delta = 57.97$ (d, $^3J_{P,C} = 4.6$ Hz), 66.13 (s), 128.40, 129.81, 133.43, 132.61 (d, $^4J_{P,C} = 8.6$ Hz; C_{ipso}), 136.91, 167.00. IR (KBr, ν, cm^{-1}): 3331 (w, br, N–H), 3265 (m, C–$H_{aromatic}$), 1651 (vs, C=O), 1432 (m, C=C), 1396 (m, C–N_{amide}), 1219 (s, P=O), 1011 (m, P–N_{amine}), 970 (w, N–N), 912 (s, P–N_{amide}), 715 (C–Cl).

Table 8
The enzymatic data for hBChE and candidate compounds.

Compound	IC_{50} (mM)	log *P*	K_m (mM)	V_m (mM/min)	Inhibition mechanism
Enzyme	–	–	0.11	40.32	–
1a	2.45	−1.12	0.067	71.43	Mixed
3a	1.62	−0.54	0.085	66.38	Mixed
7a	2.14	−0.78	0.050	23.49	Mixed
11a	0.43	1.35	0.075	55.56	Mixed
12a	1.58	1.29	0.067	27.78	Mixed

6.12. 4-Methoxy-N-benzoyl-N′,N″-bis (4-aminomorpholine) phosphoric triamide (**10a**)

Yield: 68%. M.p. = 188 °C. Anal. Calc. for $C_{16}H_{26}N_5O_5P$ (399.36): C, 48.08; H, 6.51; N, 17.53; Found: C, 48.10; H, 6.50; N, 17.60%. ^{31}P NMR (202.46 MHz, d_6-DMSO, ppm): $\delta = 2.88$ (m). ^1H NMR (500.13 MHz, d_6-DMSO, ppm): $\delta = 9.02$ (s, $^2J_{PNH} = 0$ Hz; $1H_{amide}$), 7.92 (d, $^3J_{H,H} = 8.8$ Hz, 2H; Ar–H), 6.97 (d, $^3J_{H,H} = 8.8$ Hz, 2H; Ar–H), 5.94 (d, $^2J_{PNH} = 29.6$ Hz; NH_{amide}), 3.80 (s, 3H), 3.52 (m, 8H), 2.68 (m, 8H). ^{13}C NMR (125.77 MHz, d_6-DMSO, ppm): $\delta = 27.00, 57.81$ (d, $^3J_{P,C} = 4.7$ Hz), 66.00, 113.5, 125.91, 129.91, 135.90, 162.31, 167.20. IR (KBr, ν, cm^{-1}): 3420 (w, br, N–H), 3260 (m, C–$H_{aromatic}$), 1647 (vs, C=O), 1448 (m, C=C), 1407 (m, C–N_{amide}) 1211 (s, P=O), 1173 (m, C–O), 1002 (m, P–N_{amine}), 936 (w, N–N), 910 (m, P–N_{amide}).

6.13. N-Benzoyl-N′,N″-bis (4-aminopiperidine) phosphoric triamide (**11a**)

Yield: 75%. M.p. = 204 °C. Anal. Calc. for $C_{17}H_{28}N_5O_2P$ (365.36): C, 55.83; H, 7.66; N, 19.16; Found: C, 55.80; H, 7.65; N, 19.20%. ^{31}P NMR (202.46 MHz, d_6-DMSO, ppm): $\delta = 2.49$ (m). ^1H NMR (500.13 MHz, d_6-DMSO, ppm): $\delta = 9.08$ (s, $^2J_{PNH} = 0$ Hz; $1H_{amide}$), 7.88 (d, $^3J_{H,H} = 7.8$ Hz, 2H; Ar–H), 7.48–7.69 (m, 3H; Ar–H), 5.69 (d, $^2J_{PNH} = 30.0$ Hz; NH_{amide}), 3.40 (m, 8H), 3.04 (m, 8H), 1.45 (m, 4H). ^{13}C NMR (125.77 MHz, d_6-DMSO, ppm): $\delta = 23.4$, 25.51, 58.70 (d, $^3J_{P,C} = 4.4$ Hz), 127.43, 128.11, 132.00, 134.00 (d, $^4J_{P,C} = 7.9$ Hz), 167.81. IR (KBr, ν, cm^{-1}): 3455 (w, br, N–H), 3280 (m, C–$H_{aromatic}$), 1648 (vs, C=O), 1451 (m, C=C), 1428 (m, C–N_{amide}) 1211 (s, P=O), 1017 (m, P–N_{amine}), 902 (m, P–N_{amide}), 926 (w, N–N).

6.14. Phenyl-N-(4-aminopiperidine) phosphate (**12a**)

Yield: 88%. M.p. = 128 °C. Anal. Calc. for $C_{11}H_{18}N_2O_3P$ (257.12): C, 51.34; H, 7.00; N, 10.89; Found: C, 51.39; H, 7.10; N, 10.91%. ^{31}P NMR (202.46 MHz, d_6-DMSO, ppm): $\delta = -4.49$ (s). ^1H NMR (500.13 MHz, d_6-DMSO, ppm): $\delta = 7.27$ (t, $^3J_{H,H} = 7.9$ Hz; 2H; Ar–H), 7.18 (d, $^3J_{H,H} = 7.8$ Hz, 2H; Ar–H), 6.98 (t, $^3J_{H,H} = 7.3$ Hz, 1H; Ar–H), 6.11 (br, 1H; OH), 2.99 (m, 4H), 1.66 (m, 4H), 1.34 (t, 2H). ^{13}C NMR (125.77 MHz, d_6-DMSO, ppm): $\delta = 19.71$, 21.90, 23.41, 25.60, 57.81, 128.91, 122.31, 120.10 (d, $^3J_{P,C} = 4.8$ Hz; C_{ipso}). IR (KBr, ν, cm^{-1}): 3220 (w, br, N–H), 3150 (m, C–$H_{aromatic}$), 1452 (P–Ph), 1356–1392 (w, Ph), 1171 (m, P=O), 950 (w, N–N), 876 (m, P–N_{amine}).

6.15. 4,4′-Bis(morpholine)diazene (**1b**)

Yield: 60%. M.p. = 156 °C. Anal. Calc. for $C_8H_{16}N_4O_2$ (200.12): C, 55.83; H, 7.66; N, 19.16; Found: C, 55.80; H, 7.65; N, 19.20%. ^1H NMR (500.13 MHz, d_6-DMSO, ppm): $\delta = 3.71$ (m, 8H), 3.05 (m, 8H). ^{13}C NMR (125.77 MHz, d_6-DMSO, ppm): $\delta = 49.87$, 65.31. IR (KBr, ν, cm^{-1}): 2960, 1448, 1264, 1108, 1085, 985, 857.

6.16. Dimethyl phenyl phosphonic acid (**1d**)

Yield: 68%. Anal. Calc. for $C_8H_{11}O_3P$ (186.23): C, 51.55; H, 5.91; Found: C, 51.50; H, 5.95%. ^{31}P NMR (202.46 MHz, d_6-DMSO, ppm): $\delta = 22.29$ (s). ^1H NMR (500.13 MHz, d_6-DMSO, ppm): $\delta = 7.75$ (d, $^3J_{P,H} = 6.5$ Hz, 2H; Ar–H), 7.51 (m, 1H; Ar–H), 7.43 (m, 2H), 3.71 (d, $^3J_{P,H} = 10.85$ Hz, 6H; OCH_3). ^{13}C NMR (125.77 MHz, d_6-DMSO, ppm): $\delta = 52.48$ (d, $^2J_{P,C} = 5.0$ Hz), 127.83 (d, $^1J_{P,C} = 189.0$ Hz; C_{ipso}), 128.39 (d, $^2J_{P,C} = 15.1$ Hz), 131.70 (d, $^3J_{P,C} = 8.8$ Hz), 132.48. IR (KBr, ν, cm^{-1}): 3365 (m, C–$H_{aromatic}$), 1436 (m, P–Ph), 1178 (s, P=O), 1136 (s, C–O), 791 (s, P–O).

Acknowledgement

We wish to thank the Research Council of Tarbiat Modares University for the financial support of this work.

References

[1] M.E.Y. Francisco, H.H. Seltzman, A.F. Gilliam, R.A. Mitchell, S.L. Rider, R.G. Pertwee, L.A. Stevenson, B.F. Thomas, J. Med. Chem. 45 (2002) 2708–2719.
[2] M.G. Vigorita, T. Previtera, C. Zappala, A. Trovato, M.T. Monforta, R. Barbara, F. Pizzimenti, Farmaco 45 (2) (1999) 223–235.
[3] X. Lin, I. King, M.F. Belcourt, W. Terrence Doyle, US 7,405,317B2, 2008, pp. 1–9.
[4] J. Nawrot-Modranka, E. Nawrot, J. Graczyk, Eur. J. Med. Chem. 41 (2006) 1301–1309.
[5] J. Hernandez-Lopez, H.L. Khor, A. Caminade, J. Majoral, S. Mittler, W. Knoll, D.H. Kim, Thin Solid Films 516 (2008) 1256–1264.
[6] V. Chandrasekhar, R. Azhakar, J.F. Bickley, A. Steiner, Cryst. Growth Des. 6 (2006) 910–914.
[7] M.L. Clarke, G.L. Holliday, A.M.Z. Slawin, J.D. Woollins, Inorg. Chem. Commun. 4 (2001) 115–118.
[8] M.J.P. Harger, Tetrahedron Lett. 42 (2001) 6749–6752.
[9] T.E.-S. Ali, Arkivoc ii (2008) 71–79.
[10] P.J. Blower, Annu. Rep. Prog. Chem., Sect. A: Inorg. Chem. 100 (2004) 633–658.
[11] F.M. Raushel, S.B. Hong, Biochemistry 38 (1999) 1159–1165.
[12] S.D. Cohen, R.A. Williams, J.M. Killinger, R.I. Freudenthal, Toxicol. Appl. Pharmacol. 83 (1985) 452–459.
[13] M. Jokanovic, M. Maksimovic, V. Kilibarda, D. Jovanovic, D. Savic, Toxicol. Lett. 85 (1996) 35–39.
[14] C.M. Thompson, J.A. Frick, B.C. Natke, L.K. Hansen, Chem. Res. Toxicol. 2 (1989) 386–391.
[15] M.R. Farlow, P.A. Cyrus, Dement. Geriatr. Cogn. Disord 11 (2000) 202–211.
[16] N.J. Zhang, J.E. Casida, Bioorg. Med. Chem. 10 (2002) 1281–1290.
[17] K. Law, R.A. Acey, C.R. Smith, D.A. Benton, S. Soroushian, B. Eckenrod, R. Stedman, K.A. Kantardjieff, K. Nakayama, Biochem. Biophys. Res. Commun. 355 (2007) 371–378.
[18] K. Gholivand, M. Abdollahi, F. Mojahed, A. Madani Alizadehgan, G. Dehghan, J. Enzyme Inhib. Med. Chem. 4 (2008) 1–11.
[19] K. Gholivand, A. Madani Alizadehgan, F. Mojahed, G. Dehghan, A. Mohammadirad, M. Abdollahi, Z. Naturforsch. 63c (2008) 241–250.
[20] K. Gholivand, Z. Shariatinia, K. Khajeh, H. Naderi-Manesh, J. Enzyme Inhib. Med. Chem. 21 (2006) 31–35.
[21] K. Gholivand, F. Ghaziani, R. Yaghoubi, Z. Hosseini, Z. Shariatinia, J. Enzyme Inhib. Med. Chem., in press, doi:10.3109/14756361003691860.
[22] G.L. Ellman, K.D. Coutney, V.R. Andres, M. Featherstone, Biochem. Pharmacol. 7 (1961) 91–95.
[23] R.A. Copeland, Enzymes, A Practical Introduction to Structure, Mechanism, and Data Analysis, second ed. John Wiley-VCH, New York, 2000.
[24] A.V. Kirsanov, R. Makitra, J. Gen. Chem. 26 (1956) 905–907.
[25] H. Tolkimth, Ann. N.Y. Acad. Sci. 79 (1959) 189 (Dow Chem. Co., Middland, Mich.) Art. 7.
[26] J.C. Gould, J.H. Bowie, Edinb. Med. J. 59 (1952) 178–199.
[27] K. Gholivand, M. Pourayoubi, Z. Shariatinia, H. Mostaanzadeh, Polyhedron 24 (2005) 655–662.
[28] K. Gholivand, Z. Shariatinia, S.M. Mashhadi, F. Daeepour, N. Farshidnasab, H.R. Mahzouni, N. Taheri, S. Amiri, S. Ansar, Polyhedron 28 (2009) 307–321.
[29] M. Ramaswamy, P. Ramaswamy, New J. Chem. 27 (2003) 968–974.
[30] S.H. Li, H.G. Shi, C.H. Sun, X.T. Li, S.P. Pang, Y.Z. Yu, X.Q. Zhao, J. Chem. Crystallogr. 39 (2009) 13–16.
[31] T.M. Klapçtke, P. Mayer, A. Schulz, J.J. Weigand, Propellants Explos. Pyrotech. 29 (2004) 325–332.
[32] R. Willett, H. Place, M. Middleton, J. Am. Chem. Soc. 110 (1988) 8639–8650.
[33] E.A. Trush, V.M. Amirkhanov, V.A. Ovchynnikov, V.A. Ovchynnikov, J.S. Wiatekkozlowska, K.A. Lanikina, K.V. Domasevitch, Polyhedron 22 (2003) 1221–1229.
[34] V.V. Skopenko, V.M. Amirkhanov, T.Y. Silva, I.S. Vasilchenko, E.L. Anpilov, A.D. Garnovski, Russ. Chem. Rev. 73 (2004) 737–752.
[35] O.V. Moroz, V.A. Trush, I.S. Konovalova, O.V. Shishkin, Y.S. Moroz, S. Demeshko, V.M. Amirkhanov, Polyhedron 28 (2009) 1331–1335.
[36] A. Pop, A. Rotar, C. Rat, A. Silvestru, Inorg. Chim. Acta 361 (2008) 255–261.
[37] A. Diaz, R. Cao, A. Garcia, Monatsh. Chem. 125 (1994) 823–825.
[38] D.M. Brown, N.K. Hamer, Proc. Chem. Soc. (1960) 212.
[39] R.J. Cremlin, M.J. Frearson, D.R. Milnes, Phosphorus and Sulfur 6 (1976) 207.
[40] T.G. Back, R.G. Kerr, Can. J. Chem. 60 (1982) 2711–2718.
[41] I. Bhatnagar, M.V. George, J. Org. Chem. 33 (1968) 2407–2411.
[42] J.R. Hwu, N. Wang, R.T. Yung, J. Org. Chem. 54 (1989) 1070–1073.
[43] K. Sugiyama, T. Nakaya, M. Imoto, Die Makromol. Chem 176 (2003) 587–592.
[44] W. Thun, W. Mcbride, J. Org. Chem. 34 (1969) 2997–3002.
[45] A. Sloboda, A. Vogel, Cancer Res. 24 (1964) 461–469.
[46] T.W. Schultz, M.T.D. Cronin, J.D. Walker, A.O. Aptula, J. Mol. Struct. (Theochem) 622 (2003) 1–22.
[47] M. Karelson, V.S. Lobanov, A.R. Katritzky, Chem. Rev. 96 (1996) 1027–1044.
[48] C. Hansch, W. Dunn, J. Pharm. Sci. 61 (1972) 1–19.
[49] D. Kaplan, A. Ordentlich, D. Barak, N. Ariel, C. Kronman, B. Velan, A. Shafferman, Biochemistry 40 (2001) 7433–7445.
[50] S. Riazzo, C. Riviere, L. Piazzi, A. Bisi, S. Gobbi, M. Bartolini, V. Andrisano, F. Morroni, A. Tarozzi, J.P. Monti, A. Rampa, J. Med. Chem. 51 (2008) 2883–2886.
[51] Bruker, SMART. Bruker Molecular Analysis Research Tool, v. 5.059. Bruker AXS, Madison, Wisconsin, USA, 1998.
[52] G.M. Sheldrick, Programs SHELXS97 (Crystal Structure Solution) and SHELXL97 (Crystal Structure Refinement). University of Gottingen, Germany, 1997.